https://doi.org/10.5194/bg-2022-175
Preprint. Discussion started: 29 August 2022

Biogeosciences Discussions

Post-flooding disturbance recovery promotes carbon capture in riparian zones

Yihong Zhu[3, 4#], Ruihua Liu[1,4#], Huai Zhang[1], Shaoda Liu[2], Zhengfeng Zhang[1], Feihai Yu[5], Timothy G. Gregoire[4]

[1]School of Earth and Planetary, University of Chinese Academy of Sciences, Beijing, 100049, China
[2]State Key Laboratory for Water Environment Simulation, School of Environment, Beijing Normal University, Beijing, 100875, China
[3]Department of Environmental Science, Policy and Management, University of California, Berkeley, 94704, USA
[4]Yale School of the Environment, Yale University, New Haven, 06511, USA
[5]Institute of Wetland Ecology & Clone Ecology; Zhejiang Provincial Key Laboratory of Plant Evolutionary Ecology and Conservation, Taizhou University, Thaizhou, 318000, China
[#]Yihong Zhu and Ruihua Liu contributed equally to this paper.

Correspondence to: Shaoda Liu (liushaoda@bnu.edu.cn); Huai Zhang (hzhang@ucas.ac.cn)

Abstract. Vegetation, water, and carbon dioxide have complex interactions on carbon mitigation in vegetation-water ecosystems. As one of the major global change drivers of carbon sequestration, water disturbance is a fundamental but poorly discussed topic to date. The riparian zone is a representative highly dynamic vegetation-water carbon capture system. Unfortunately, its global carbon offset functionality is remarkably underestimated. This study examines the daily CO_2 perturbations in the riparian zone with two-year in-situ observations along the Lijiang River. We show that the riparian zone transformed from a carbon source to carbon sink after recovery from flooding. Consequently, a quantitative global riparian carbon offset model is proposed. Based on the intensity of flooding submergence and post-flooding vegetation coverage, ~0.11Gt·year^{-1} CO_2 is captured following flooding, and 0.53 Gt·year^{-1} more CO_2 is captured due to flooding, which is equivalent to 9.1 % of the global forest carbon sequestration. This finding shed new light on the quantitative modelling of the riparian carbon cycle under flooding disturbance, underlining the importance of the proper restoration of riparian systems to achieve global carbon offset.

1 Introduction

Climate change issues stemming from carbon emissions have strengthened dramatically, immensely threatening ecosystem stability and biodiversity (Li et al., 2022; Wang et al., 2020). The increasing atmospheric CO_2 originating from fossil fuel combustion and industrial activities can be regulated by plant metabolism (photosynthesis and respiration) and soil microbial activities (Xunhua et al., 1998). In general, the net carbon emission strongly depends on the balance between the production and consumption processes in the vulnerable natural ecosystem (Pugh et al., 2019).

https://doi.org/10.5194/bg-2022-175
Preprint. Discussion started: 29 August 2022

Aquatic and terrestrial systems are highly dynamic systems driven by fluvial processes (ex: flooding and deposition of alluvial soil) (Naiman and Decamps, 1997; Steiger et al., 2005). Riparian zones are generally defined as a complex terrestrial assemblage of plants and other organisms adjacent to an aquatic environment. For instance, the interface between aquatic and terrestrial environments in coniferous forests forms a narrow riparian zone (Gregory et al., 1991). Flooding is one of the most common forms of environmental disturbance in riparian zones, which strongly influences the biotic characteristics of riparian assemblages (Anderson et al., 2020). Floods can be natural, but human activity such as the construction of dams increasingly causes controlled floods (Darrel Jenerette and Lal, 2005; Dynesius and Nilsson, 1994). Variations in riparian vegetation communities are expected to define the ecological role of riparian zones in carbon cycle. Flooding submergence may impede gas diffusion and decrease light intensity, leading to high mortality and limited plant individuals (Colmer et al., 2009). This raises the possibility that riparian zones may promote carbon emission, shifting the role of riparian zones from carbon sink to the carbon source. It is supported by the fact that the rate of CO_2 emission in riparian wetlands is higher than that in neighbouring hillslope grasslands (Anderson et al., 2020).

Disturbances in vulnerable ecosystems like riparian zones may change the system from carbon sinks to carbon sources (Running, 2008). Disturbances have the potential to both augment and offset the carbon loading of the atmosphere attributed to anthropogenic carbon emissions (Sierra et al., 2017). Carbon capture can be promoted by lengthening the growing season and expanding the niches from which water can be drawn (Mahanta et al., 2020). On the contrary, carbon emission can be promoted by pervasive growth-lifespan trade-offs as it happens in forests (Brienen et al., 2020; Gatti et al., 2021). Since three-quarters of disturbances are directly human-induced (Venter et al., 2016), a better understanding of the role of disturbance on vegetation in the carbon cycle is highly relevant to reducing carbon emission (Pugh et al., 2019).

The indispensable role of riparian vegetations in sequestering carbon is increasingly underlined in the context of global climate change (Maraseni and Mitchell, 2016). Riparian vegetations are often considered as sinks for CO_2 through the pathway of photosynthetic assimilation of CO_2 and carbon sequestration in soil under anaerobic conditions. They are also a potential CH_4 source in the natural environment (Hassanzadeh et al., 2019; Hondula et al., 2021; Morse et al., 2012). Liu et al. (2021) demonstrated that high plant and soil respiration in riparian wetlands may lead to larger amounts of CO_2 emission than CH_4 detected in the wet season (wet season: 335-2790 $mg \cdot m^{-2}h^{-1}$; dry season: 72-387 $mg \cdot m^{-2}h^{-1}$) (Liu et al., 2021). Conversely, as riparian species recover after flooding, riparian zones can promote CO_2 capture. Considering different types of water fluctuations, Hirota et al. (2007) compared three greenhouse gas fluxes in the sandy shore and salt marsh of a coastal lagoon in Japan. They find that temporal variations of the fluxes are strongly manipulated by water-level fluctuations in the salt marsh's sandy shore and soil temperature (Hirota et al., 2007). Therefore, riparian zones oscillate between a carbon source and sink depending on flooding. It raises the open question of whether riparian zones quantitatively promote or hinder carbon capture overall.

https://doi.org/10.5194/bg-2022-175
Preprint. Discussion started: 29 August 2022

Overall, the riparian zone is believed to have considerable potential to contribute to biodiversity, carbon sequestration, and several other ecosystem services. As a traditional practice, it has been cleared for crop and pasture production in numerous places worldwide, leading to greenhouse gas emissions increase (Maraseni and Cockfield, 2011). It is noteworthy that proper and efficient restoration of the riparian zones is fundamental. Thus, it has been listed as a priority in the Intergovernmental Panel on Climate Change (IPCC) community (Bullock et al., 2011). Unfortunately, the current research on the carbon offset contribution of riparian zone remains poorly constrained with a quantitative measure to date.

In order to figure out how floods affect the balance between the carbon emission and carbon capture in riparian areas, we quantified the effect of flooding disturbance on riparian carbon cycle. Based on two-year in-situ measurements along the Lijiang River, we analysed the vertical CO_2 fluxes at the soil-air interface and water-air interface during the dry seasons and the wet seasons. We establish that a riparian system promotes carbon capture despite transient phases of carbon emission. Its capacity is directly correlated to the vegetation density, especially on the resilience of post-disturbance recovery. It indicates that promoting the recovery of riparian systems and establishing high flooding-tolerant vegetation coverage is key to promoting carbon capture in the context of global change. Therefore, this work reveals how water disturbance affects the balance between carbon emission and carbon sequestration in water-vegetation diverse areas. It quantitatively estimates the effect of flooding disturbance on riparian carbon dynamics. Eventually, we build a quantitative riparian carbon offset model based on the disturbance intensity and post-vegetation coverage to evaluate the global carbon change due to flooding.

2 Methods

2.1 In-situ observation setup

Our study site is located in the riparian zone, downstream of the 164 kilometres long Lijiang River in the Pearl River Basin in northwestern Guangxi Zhuang Autonomous Provence, Southwest China (25° 06′ N, 110° 25′; Fig. A1). This area experiences a monsoon-based humidity subtropical climate, where the mean annual rainfall is 1900 mm, and the annual temperature ranges from 7.9 to 28.0 °C. In the dry season (normally September to March next year), the minimum daily average flow discharge is often below 20 m^3/s. Therefore, drought stress profoundly influences the early-stage development of riparian species. By contrast, in the flooding season (April to August), discharges over 1000 m^3/s are common during flood events, inner islands are completely submerged, and some riparian species cease to grow or are destroyed.

2.2 Experiment design

2.2.1 Gas collection

Four transects are established on one island downstream of the Lijiang River (Fig. A1). The distance between each transect is approximately 3 m. Four subplots spaced 5-8 m apart are deployed in each transect, perpendicular to the waterlines and

https://doi.org/10.5194/bg-2022-175
Preprint. Discussion started: 29 August 2022

extended from the edge of the water body to the upper area. CO_2 in four 50 x 50 cm subplots along each transect are sampled by static chamber techniques (length 50 cm, width 50 cm, and height 50 cm) with two exhaust fans, a thermometer, and a tube for collecting gas samples. The chamber is insulated from rapid temperature changes by a foam covering and reflective aluminum. The underside portion, made from stainless steel (50 cm in length, 50 cm in width, and 15 cm in height), is created to increase the chamber's size and prevent damage to the vegetation inside. Four static chambers are used at each site. Chambers remain in the same subplots representing typical seasonal grass-based hyporheic zones and are subject to seasonal fluctuation. CO_2 fluxes are sampled pre-flooding season, during flooding season, and post-flooding season from 2014 to 2016. Four repeated static chambers are used at each site with and without vegetation, and chambers are positioned in the same location for the duration of the monitoring phase.

2.2.2 Vegetation inventory and flooding tolerant experiment

Vegetation inventory is conducted by three 15 m x 5 m transects along with this field site. Coverage, number of ramets, and height are measured. After the field inventory, about 300 seeds of the dominant riparian species after flooding, *C. aciculatus* are sown in planting trays filled with peat (Pindstrup Seeding; Pindstrup Mosebrug A/S, Pindstrup, Denmark). Seeds are bought from Forest Science Co, Ltd. of Beijing Forestry University. Eight grass plants with one single ramet are transplanted in the experimental pots. In total, 178 ramets with similar sizes of each species are selected for the experiment, of which 18 are randomly used to obtain their initial length and dry mass, and the remaining 80 ramets are used for the experiments. The initial ramet length of *C. aciculatus* is 9.56 ± 0.18 cm, and the dry mass is 38.56 ± 5.36 mg. The experiment lasted three months, from August 01 to November 01. The mean temperature and relative humidity are 26.21 ± 0.33 °C and 59.02 ± 1.46%, respectively. Sufficient tap water is added to each container to maintain the plant submerged in the water. At harvest, new ramets produced by each initial one are interconnected by aboveground stolon, so we can harvest and measure the growth attributes of plants in each treatment separately. We count the number of ramets and weigh each plant's dry leaf, rhizome, and biomass in each container. All plant parts are oven-dried at 70°C for 72 h before weighing. The collection of materials complies with relevant institutional, national, and international guidelines and legislation.

2.2.3 Measurement of gas concentration and hydro-environment condition

Diel data are taken at every four hours base (6 times per day starting at 10:00 and finishing at 06:00 the next day). Gas samples are collected in airtight glass bottles. All samples are analyzed within three days, using Agilent7890A gas chromate. The calculation formula of CO_2 flux is

$$F = \frac{M}{V_0}\frac{P}{P_0}\frac{T_0}{T} H \frac{dc}{dt} \quad (1)$$

where F represents the gas flux ($\mu g \cdot m^{-2} h^{-1}$), M is the molar mass, V_0 represents the normal state of molar volume (22.4 L/mol), P_0 and T_0 are the pressure and temperature of the standard conditions (1013.25 hPa, 273.15 K) for gases, and d_c/d_t is the slope of the regression curve as gas concentration variable with time, respectively. The height of the chamber (H, cm),

https://doi.org/10.5194/bg-2022-175
Preprint. Discussion started: 29 August 2022

in-situ air pressure (P, hPa), and air temperature (T, K) are recorded during the sampling as well. The all-day CO_2 flux is calculated by integrating the diel CO_2 flux of different measuring times. The environmental information, including total organic carbon (TOC) and total inorganic carbon (TIC) (from April 01 to October 01 in 2014 and 2016) downstream (Yangshuo Gauge) of the Lijiang River, is also recorded (Fig. A2). Meanwhile, the water level is recorded hourly during the experiment period. Site selection and chamber placement minimized differences in the microclimate among chamber stations (Fig. A1).

2.2.4 Data analysis

For terrestrial habitats, two-way repeated-measures ANOVAs are employed to examine the effects of vegetation (bare soil vs. land with vegetation; between-subject factor) and time (measuring times in one day, within-subject factor) on the CO_2 flux in two sampling stages (April: pre-flooding and October: post-flooding). For aquatic habitats, two-way repeated-measures ANOVAs are used to examine the effects of sampling position (with vegetation vs. without vegetation or under water surface; between-subject factor) and time (measuring times in one day; within-subject factor) on CO_2 flux in sampling stages (April: pre-flooding, August: during flooding, and October: post-flooding). The *p*-values are calculated with the null hypothesis that the CO_2 flux of terrestrial or aquatic habits is not influenced by the factors mentioned. Before analyses, homogeneity of variance and normality are also examined. All data analyses are performed by the SPSS statistical software package (https://www.ibm.com/products/spss-statistics, version 22.0, Chicago, IL, USA). The effects are considered significant if p-value < 0.05.

2.3 Model scenario prediction method

2.3.1 Riparian carbon offset model

The carbon cycle considered in this model consists of the carbon flux of the terrestrial riparian zone (with bare soil and with vegetation) and the carbon flux of the river. Flooding events influence it in summer. We assume that flooding events happen at an annual timescale and consider the time that flooding would happen as flooding season. The area of the terrestrial riparian zone in this model refers to the area submerged during flooding. This model assumes that the terrestrial riparian zone in the dry season is 25% of the river width in the flooding season. We also assume the whole river to be a homogenously mixed reactor, so do not vary river morphometry. We do not consider the water temperature and the occurrence of extreme weather like rainstorms or frost.

The riparian carbon offset model is given as

$$C = \int_{p=0}^{1} D_\theta\,(p)\,\mathrm{d}p \quad (2)$$

where C is the annual expected carbon emission (C=0 when reaches carbon neutralization), D is an impact or disturbance model, potentially consisting of both direct and indirect, tangible, and intangible components associated with flooding, along with certain event characteristics such as flood levels, extents, and durations, with an annual probability of non-exceedance p

https://doi.org/10.5194/bg-2022-175
Preprint. Discussion started: 29 August 2022

[1/T]. Finally, p represents a vegetation coverage of fixed-in-time factors, determining the vulnerability. Such factors eventually determine the shape of D. In brief, D_θ combines the exposure and vulnerability within an area into a disturbance function. The consequence D_θ of the event with vegetation coverage p can be expressed in a plethora of indicators, reflecting for disequilibrium of carbon neutralization. The associated vulnerability determining factors, θ, may differ depending on the type of consequence used to estimate them. The parameters used in this study can evaluate the carbon offset for rivers with similar biogeochemical characteristics as the Lijing River in southern China. Nonetheless, the specific parameter related to river length, river width, vegetation coverage rate, and carbon flux needs to be measured to develop other rivers' parameters.

2.3.2 Global riparian carbon emission scenario prediction method

To compare the CO_2 flux after flooding disturbance and the CO_2 flux of global forests, the global forest coverage and CO_2 flux are obtained from Harris (Harris et al., 2021). The vector shapefile of the Global River Widths from Landsat (GRWL) Database is used to map the global riparian CO_2 that can be fixed after flooding disturbance (Allen and Pavelsky, 2018a, b). The total surface area of rivers that are wider than 90 m, where GRWL data are the most complete and accurate, is about 404,000 km^2 (Allen and Pavelsky, 2018a).

3 Results

3.1 Vegetation overall promotes carbon capture despite a transient carbon release during the pre-disturbance nights

In order to evaluate whether riparian vegetation promotes carbon emission or sequestration, we directly measured the CO_2 fluxes in the riparian area with and without vegetation (bare soil) at different seasons. Because daylight promotes photosynthesis, the first level we reviewed is the diel cycle. Significant diel variations in CO_2 fluxes were observed in the terrestrial area in both pre-flooding season and post-flooding season (April: low water level before flooding; October: resumed low water level after flooding; Table 1). Within a day, the carbon sequestration in the riparian area with vegetation peaked at 10:00 in April and at 14:00 in October (April: -87.89 $mg \cdot m^{-2} h^{-1}$; October: -104.33 $mg \cdot m^{-2} h^{-1}$); and the maximum carbon emission occurred at 18:00 (April: 61.49 $mg \cdot m^{-2} h^{-1}$; October: 34.75 $mg \cdot m^{-2} h^{-1}$; Fig. 1). However, the time periods that the terrestrial area with vegetation functions as carbon sink differ in pre-flooding and post-flooding season. In April, carbon sequestration in the terrestrial area with vegetation is observed between 10:00 to 14:00 hours; while in October, the carbon sequestration is observed between 6:00 to 14:00 hours (Fig. 1). Thus, in post-flooding season, the terrestrial area with vegetation sequestrates carbon for a longer time. Indeed, the vegetation area's all-day CO_2 flux is 0.358 $g \cdot m^{-2} d^{-1}$ in April but is -0.680 $g \cdot m^{-2} d^{-1}$ in October, transferring from a carbon source to a carbon sink. In other words, without submergence, the riparian vegetation may cause more carbon emissions than bare soil at night (than during the day) and function as a carbon source on diel level. Therefore, even though the all-day CO_2 flux of bare soil changed from -0.927 $g \cdot m^{-2} d^{-1}$ to -0.231 $g \cdot m^{-2} d^{-1}$, showing a reduced capacity of carbon sequestration, the whole terrestrial area still turns out to be a carbon sink in the post-flooding season.

https://doi.org/10.5194/bg-2022-175
Preprint. Discussion started: 29 August 2022

Averaging the CO_2 flux of bare soil and vegetation land, we can get the CO_2 flux of terrestrial area in the riparian zone. In both April and October, the all-day carbon fluxes in the riparian terrestrial area are negative, indicating that the riparian zone acted overall as a carbon sink (April: -0.284 $g \cdot m^{-2} d^{-1}$, October: -0.454 $g \cdot m^{-2} d^{-1}$). Within a day, the carbon sequestration in the riparian terrestrial area peaked at 14:00 (April: -73.688 $mg \cdot m^{-2} h^{-1}$; October: -59.810 $mg \cdot m^{-2} h^{-1}$), and the maximum carbon emission occurred at 18:00 (April: 30.129 $mg \cdot m^{-2} h^{-1}$; October: 9.084 $mg \cdot m^{-2} h^{-1}$; Fig. 1).

Since the flux of riparian terrestrial area measured fluxes from both soils below and the vegetation above in area with vegetation, we subtracted the CO_2 flux of bare soil from the CO_2 flux of the area with vegetation to measure how the cover of vegetation improve or reduce the carbon sequestration. In April, the difference between riparian area with and without vegetation is 0.128 $g \cdot m^{-2} d^{-1}$, indicating that vegetation cover actually reduces carbon sequestration and contributes to carbon emission. In October, the difference is -0.453 $g \cdot m^{-2} d^{-1}$, indicating that the capacity of vegetation to fix carbon also improves after submergence. Thus, even though the all-day CO_2 flux of bare soil changed from -0.927 $g \cdot m^{-2} d^{-1}$ to -0.231 $g \cdot m^{-2} d^{-1}$, showing a reduced capacity of carbon sequestration after flooding, the whole terrestrial area still turns out to be a carbon sink in the post-flooding season. In all, we found that in the post-flooding season, the riparian vegetation can sequestrate carbon dioxide for a longer time and fix more carbon.

Table 1. Repeated measures ANOVAs for effects of vegetation (bare soil without vegetation vs. with vegetation; between-subject factor) and time (measuring times in one day; within-subject factor) on the CO_2 fluxes in two sampling stages (April and October) in terrestrial habitats. Degree of freedom, *F*, and *P* (significance) values.

Sampling stages	Effects	df	*F*	*p-value*
April	Vegetation (V)	1,8	**102.506**	**<0.001**
	Time (T)	5,40	**22.411**	**<0.001**
	T x V	5,40	**12.909**	**<0.001**
October	Vegetation (V)	1,8	**61.47**	**<0.001**
	Time (T)	5,40	**9.25**	**<0.001**
	T x V	5,40	**5.959**	**<0.001**

F value: the ratio of two estimates of the variance between or within groups in ANOVAs;

P-value: the probability of the *F* value in the *F* distribution. The *p*-values were calculated under the null hypothesis that CO_2 flux is not influenced by the existence of grass or measuring times in terrestrial habitats.

https://doi.org/10.5194/bg-2022-175
Preprint. Discussion started: 29 August 2022

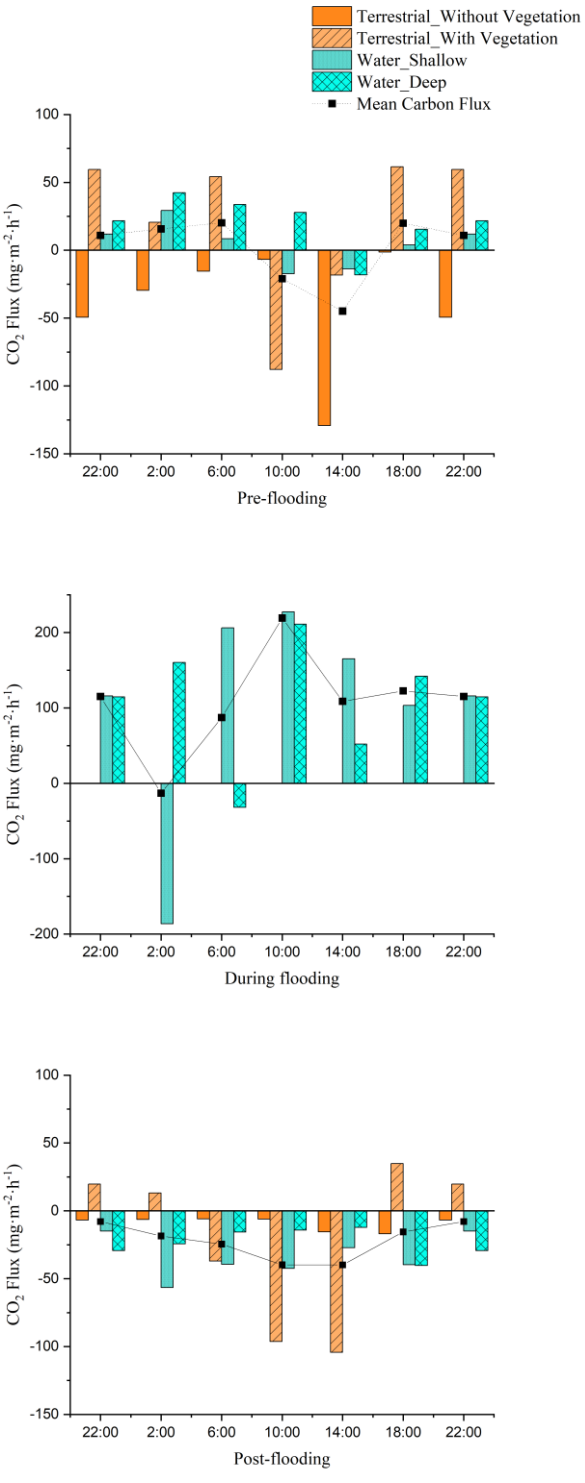

Figure 1. CO_2 fluxes in terrestrial area (with vegetation and without vegetation) and water area (shallow and deep) in April (pre-flooding), August (during flooding), and October (post-flooding).

https://doi.org/10.5194/bg-2022-175
Preprint. Discussion started: 29 August 2022

3.2 Flooding causes transient carbon emission in fluvial zones, which begins to sequestrate carbon in post-flooding season

Since pre- and post-flooding vegetations are linked to different carbon fluxes, we seek to determine the contribution of flooding itself to carbon fluxes. During the flooding, the terrestrial area with and without vegetation are submerged, so the only carbon flux we measured is the water-air carbon flux. All the riparian water-air CO_2 flux is calculated as the mean of the CO_2 flux in deep water and shallow water. By analysing and calculating the all-day CO_2 flux, we find that the fluvial area turned from a carbon source to a carbon sink. In 2014 and 2016, the riparian water surface appeared to be carbon sources before and during flooding, with a carbon flux ranging from 0.291 $g \cdot m^{-2} d^{-1}$ to 4.678 $g \cdot m^{-2} d^{-1}$ (Fig. 2, Table 2). However, after flooding, the river become a carbon sink. The all-day CO_2 fluxes are -0.712 $g \cdot m^{-2} d^{-1}$ and -0.526 $g \cdot m^{-2} d^{-1}$ in 2014 and 2016, respectively (Fig. 2, Table 2). Thus, after flooding, both the terrestrial area and the water area turns out to be a carbon sink.

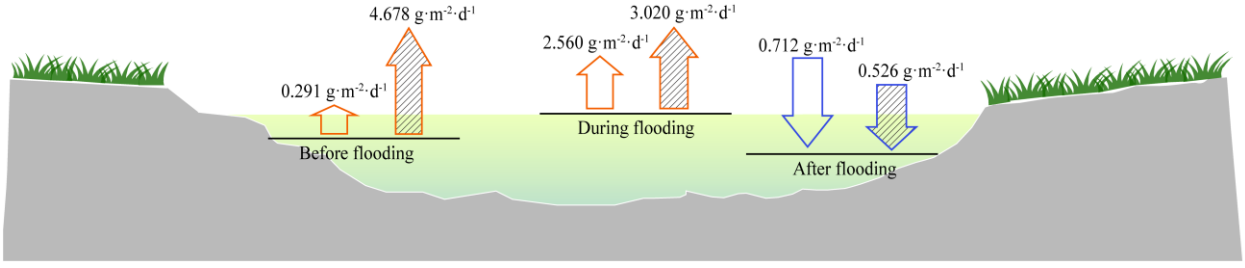

Figure 2. All-day CO_2 flux with low water-level before flooding, high water-level during flooding, and resumed low water-level after flooding in 2014 (Blank) and 2016 (Filled). The upward arrow refers to carbon emission, and the downward arrow refers to carbon uptake.

Table 2. Repeated measurements ANOVAs for effects of sampling position (water surface with vegetation vs. without vegetation; between-subject factor) and time (measuring times in one day; within-subject factor) on CO_2 fluxes in three sampling stages (April, August, and October) in aquatic habitats. Degree of freedom (*df*), *F*, and *P* (significance) values are given.

Sampling stages	Effects	*df*	*F*	*p-value*
April	Position (P)	1,4	0.003	0.956
	Time (T)	5,20	**4.306**	**0.008**
	T x P	5,20	**7.431**	**<0.001**
August	Position (P)	1,4	0.003	0.956
	Time (T)	5,20	**4.306**	**0.008**
	T x P	5,20	**7.431**	**<0.001**
October	Position (P)	1,4	7.484	0.052

https://doi.org/10.5194/bg-2022-175
Preprint. Discussion started: 29 August 2022

	Time (T)	5,20	2.183	0.097
	T x P	5,20	**6.552**	**0.001**

F value: the ratio of two estimates of the variance between or within groups in ANOVAs; *P*-value: the probability of the *F* value in *F* distribution. The *p*-values were calculated under the null hypothesis that CO_2 flux is not influenced by sampling positions or measuring times in aquatic habitats.

3.3 Flooding transiently decreases vegetation diversity and promotes the establishment of new dominant species

Vegetation plays an essential role in the carbon sequestration of riparian area. Since vegetation-related carbon fluxes differ pre- and post-flooding, we hypothesized that the established species also differed, potentially leaving space for species that are more apt at capturing carbon. We observed that species richness is severely disturbed after flooding. The species richness index decreased from 2.945 before flooding to 1.695 after flooding (Table 3). The dominant species also changed. Before the flooding, *Cynodon dactylon* (Linn.) Pers. was dominant, having wide distribution and high coverage in the riparian zones. After flooding, *Chrysopogon aciculatus* (Retz.) Trin. (*C. aciculatus*) and *Polygonum lapathifolium* L. are prevalent in surviving species (Table 3). In the 90-day submergence-controlled experiment, *C. aciculatus* also survived, showing good tolerance of submergence. However, individual biomass and the number of *C. aciculatus* both decreased (Fig. 3).

Table 3 The species richness and dominant species change from pre-flooding (April) to post-flooding (October).

	Species number	Species richness index	Dominant species	Average coverage of dominant species (%)
Pre-flooding	13	2.945	*Cynodon dactylon*	28.61
Post-flooding	7	1.695	*Chrysopogon aciculatus*	28.75

https://doi.org/10.5194/bg-2022-175
Preprint. Discussion started: 29 August 2022

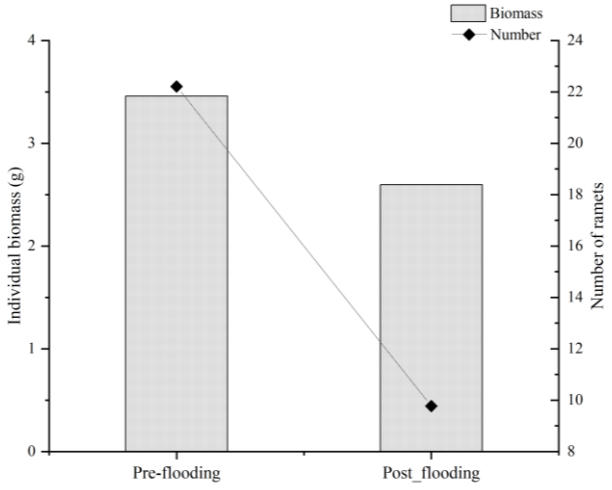

Figure 3. The comparison of the individual biomass and number of *Chrysopogon aciculatus* before and after flooding in the controlled experiment.

3.4 Vegetation density defines carbon sequestration capacity in riparian habitats

Having established that flooding cycles disturb carbon fluxes but overall promote carbon sequestration, we explore the factors that would allow greater sequestration. For that purpose, we measured mobilized carbon in the habitat using Total Organic Carbon (TOC) and Total Inorganic Carbon (TIC).

TOC in the water surface changes seasonally, but it is not affected by water habitat (Fig. A2a). TOC in April and October is significantly lower than in August (Fig. A2a). By contrast, season and water habitat significantly alter TIC in the water surface (Fig. A2b). TIC in April and October are substantially higher than that in August (Fig. A2b). TIC in April and October are also significantly higher in the deep water region without submerged vegetation than in the shallow water region with submerged vegetation. In contrast, TIC in August is not affected by water habitat (Fig. A2b).

TOC and TIC in the terrestrial area are significantly affected by season and riparian habitat (Fig. A2c and d). They are considerably higher in October than in April (Fig. A2c and d). TOC in October remarkably increases in the terrestrial area with vegetation than without vegetation. Still, TIC in October is significantly higher in the riparian area without vegetation (Fig. A2c and d). The terrestrial habitat does not change TOC and TIC in April. Those results indicate that overall, more vegetation allows capture of more carbon, although whether the carbon is stored in organic or inorganic form depending on a variety of factors.

https://doi.org/10.5194/bg-2022-175
Preprint. Discussion started: 29 August 2022

3.5 A carbon offset model shows that Lijiang riparian zones act as carbon sink after flooding but overall, a carbon source

Based on the riparian carbon offset model in Sect. 2.3.1, we assume that when C=0, the riparian zone would achieve carbon neutralization (Fig. 4). Under the assumption of carbon neutralization, the relationship between the flooding days and the post-disturbance vegetation coverage required to achieve carbon neutralization can be revealed. For example, using the carbon flux measured in Lijiang River in this study, we found that the riparian zone can only achieve carbon neutralization when flooding days are fewer than 15 days, assuming the post-disturbance vegetation coverage in the dry season is about 60%. Since the flooding season can hardly be only 15 days, the Lijiang riparian zone is overall a carbon source at the yearly level and cannot reach carbon neutralization. This is mainly due to the high carbon emission during flooding. The flooding days in Lijiang River are about 80 days, assuming the river width is 175m and the vegetation coverage to be 60%, the net CO_2 flux in Lijiang River is 35.75 $kg \cdot m^{-1} \cdot year^{-1}$. Though the recovered vegetation help fix 3.29 $kg \cdot m^{-1}$ more CO_2 after flooding, the carbon emission during the flooding season achieves 39.06 $kg \cdot m^{-1}$. Also, besides the contribution of recovered vegetation, our data shows that bare soil also contributes to the carbon neutralization, but the mechanism for bare soil to capture carbon still needs further soil chemistry analysis. Flooding days and post-flooding days are also essential factors for the carbon offset model, future detailed measurements are required to monitor the carbon dynamics of the riparian zone.

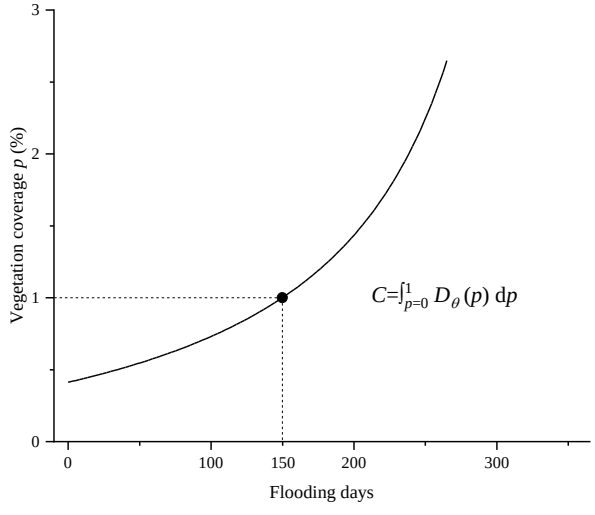

Figure 4. One possible diagram for the relationship between flooding days and post-disturbance vegetation coverage to reach carbon neutralization (C=0) in the riparian zone on an annual basis.

3.6 Disturbance in riparian zones significantly contributes to global carbon sequestration

After flooding disturbance, the riparian water surface becomes a carbon sink from a carbon source with a CO_2 flux of -0.62 $g \cdot m^{-2}\ d^{-1}$, about 1.58 times the CO_2 flux of global forests (-0.39 $g \cdot m^{-2}\ d^{-1}$) (Harris et al., 2021). The riparian zone has a higher

https://doi.org/10.5194/bg-2022-175
Preprint. Discussion started: 29 August 2022

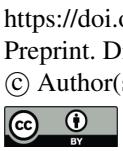

efficiency in capturing CO_2 than forests. The global CO_2 fixed by river after flooding disturbance reaches 0.11 Gt per year. After flooding disturbance, the water surface of riparian zone fixs 0.53 Gt more CO_2 compared with pre-flooding season, which is about 9.1 % of the CO_2 fixed by the global forests. Proper restoration of the riparian zone after flooding disturbance can greatly contribute to global carbon offset (Fig. 5).

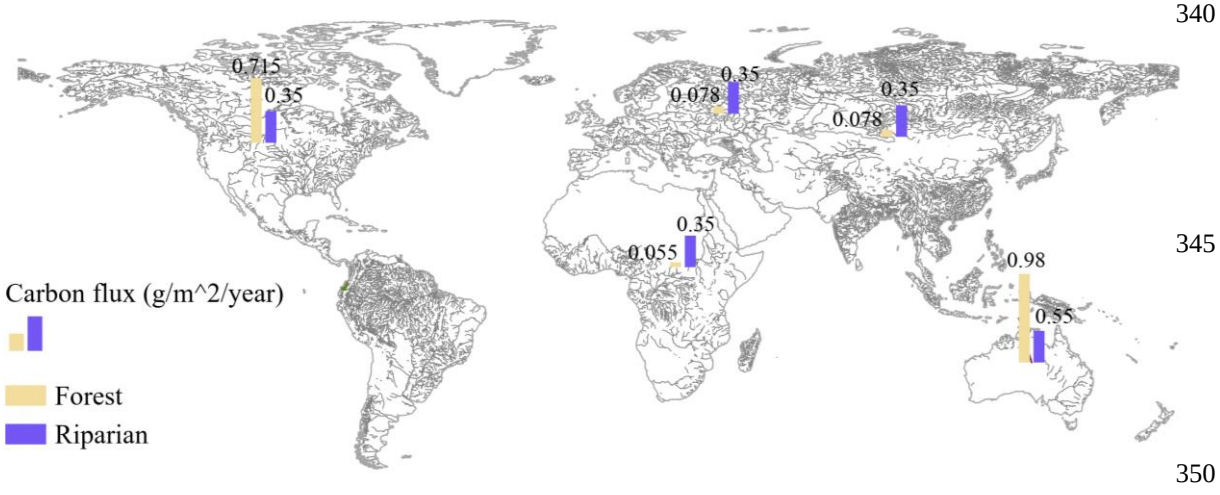

Figure 5. Carbon fluxes in forests and riparian zones of Asia, North America, Europe, Africa, and Australia. The riparian carbon flux for each continent is estimated by data collected in this study. Combining the riparian carbon flux data with flooding days, days of winter and fall, and continental riparian area, one can calculate the total carbon flux for each continent. The forest carbon flux is collected from previously published papers and authoritative online resources. The riparian carbon flux is higher than forest carbon flux in Asia, Europe, and Africa, showing great potential in carbon offset.

4 Discussion

The present work demonstrates significant variations in spatial and temporal carbon flux from riparian zones. In April, the average CO_2 fluxes are positive on the daily scale in aquatic habitat, indicating a net emission from the water to the atmosphere. However, opposite results are found for the CO_2 flux in October after the flooding disturbance, which more than offsets the previous carbon emission. Finally, we find that the carbon sequestration capacity of a given system depends strongly on disturbance duration and vegetation cover, especially on the vegetation resilience of post-flooding recovery.

https://doi.org/10.5194/bg-2022-175
Preprint. Discussion started: 29 August 2022

4.1 Post-disturbance survived vegetation is a critical factor that allows riparian systems to change from carbon source to carbon sink after flooding

We observed that the carbon sequestration of riparian zone was greatly enhanced after the flooding period, to the point that the overall carbon flux was negative. Kathilankal et al. (2008) also proposed that tidal inundation caused a mean reduction of 49 % in the marsh-atmosphere carbon (CO_2) flux compared to non-flooded conditions (Kathilankal *et al.*, 2008). Our study offers proof that the hydrological flow is a determining factor on whether the ecosystem is a net carbon source or sink. One possible reason is that the vegetation's recovery after flooding enhances its ability to sequestrate more CO_2 for photosynthesis. Still, the succession of vegetation we observed after flooding suggests that not all plants can survive submergence and to be as efficient as carbon sinks. Indeed, species richness decreased after flooding, which indicates a decrease of the interspecific competition, giving a chance to species that can quickly recover from submergence. The dominant species changed from *C. dactylon* to *C. aciculatus* after flooding disturbance. Although the individual biomass and number of *C. aciculatus* do not increase, existing literature suggests that the leaf maximum net photosynthesis rate may increase significantly after severe submergence in the riparian zones of Lijiang (Huang *et al.*, 2017, Jie *et al.*, 2012). For the clonal plants, its physiological integration allowing them to survive submergence and spread rapidly after de-submergence. Luo et al. (2014), studying *Alternanthera philoxeroides* (alligator weed) after 30 days of submergence, found that connections between submerged and non-submerged ramets enhance the performance of the submerged ramets; and the de-submerged ramets had high soluble sugar concentrations, suggesting high metabolic activities (Luo et al., 2014). Wei et al. (2018) also found that after 30 days of submergence, stolon connection significantly increased growth, biomass allocation to roots and photosynthetic capacities of the submerged ramets, and increased growth and photosynthetic capacities of the un-submerged ramets (Wei et al., 2018). Also, flooding could promote CO_2 use efficiency and the ability of the plant to use low light (Wang et al., 2019). The enhanced photosynthetic capacity is believed to be one of the physiological strategies for species growing in critical zones with flooding disturbance. Moreover, human impacts can no longer be ignored on the riparian ecosystem (Ren et al., 2019), suggesting vegetation that can recover quickly and densely is essential to allow riparian zones to be efficient carbon sinks.

Our data also shows that vegetation land before flooding can be a carbon source. This perhaps because the role of vegetation as a substrate source through litter production and root exudates can vary among species (Hirota et al., 2007). Previous work also reported that the extensive root system of riparian species with strong taproots and well-developed fibrous roots could force the species to demand more oxygen and accelerate root respiration and CO_2 emissions from the neighbouring rhizosphere (Elias et al., 2015). In submerged areas, the CO_2 may be emitted to water and then released to the atmosphere as the carbon flux of water surface. Especially, the recovery of some C_4 riparian species after periodic flooding also contributed to the higher gas transportability and abundant substrate for CO_2 emission compared to the performance of C_3 species (Still et al., 2003). Research should be directed towards understanding how plants such as *C. aciculatus* can colonize flooded riparian zones efficiently and promoting plants with similar characteristics in restoration efforts.

https://doi.org/10.5194/bg-2022-175
Preprint. Discussion started: 29 August 2022

When comparing the CO_2 flux of shallow-water area (with aquatic vegetation) and deep-water area (with no vegetation) (Fig. A3), it is also found that shallow-water releases less carbon in pre-flooding season and captures more carbon in post-flooding season than deep-water area (pre-flooding: 0.090 $g \cdot m^{-2} d^{-1}$ in shallow water, 0.492 $g \cdot m^{-2} d^{-1}$ in deep water; post-flooding: -0.880 $g \cdot m^{-2} d^{-1}$ in shallow water, -0.545 $g \cdot m^{-2} d^{-1}$ in deep water). However, during the flooding season, both the shallow-water and deep-water areas have carbon flux of about 2.55 $g \cdot m^{-2} d^{-1}$, probably because during flooding no aquatic vegetation was able to fix carbon through photosynthesis.

4.2 Flooding disturbance leads to transiently increasing carbon emission, which cannot be offset by post-disturbance recovery

During the flooding period, the carbon emission of water area significantly increases and shows a net emission of CO_2 in both the daytime and night-time (all-day CO_2 flux: 0.291 $g \cdot m^{-2} d^{-1}$ in April, 2.560 $g \cdot m^{-2} d^{-1}$ in August). This is probably due to the increased lateral carbon flux from terrestrial areas to rivers due to flooding. Research found that when water flows through ecosystem, it would pick up dissolved organic carbon (DOC) from vegetation and soils, transporting DOC from terrestrial ecosystem to streams. When the water is flowing fast, more carbon would be transported out of the watersheds. Zarnetske et al. (2018) found that in 80% of the watersheds of United States the hydrologic flow determined the DOC flux behaviour (Zarnetske et al., 2018).

Using the carbon offset model, the result shows that even with 100% vegetation coverage, the whole riparian zone can hardly achieve carbon neutralization at yearly level when the flooding days are higher than 15. This is mainly due to the high carbon emission during flooding. Nowadays, with global warming, the risk and the number of global flooding events are also rising (Hirabayashi et al., 2013), meaning that the carbon cycle of riparian zone are more dynamic than ever. Based on 11 climate models, previous research projects found that with a warmer climate, there would be a large increase in flood frequency in Southeast Asia, Peninsular India, eastern Africa and the northern half of the Andes (Hirabayashi et al., 2013). Our research highlights that flooding disturbance would not only cause large carbon emission during the flooding season, but can also promote carbon sequestration in the post-flooding season. It is necessary to consider the dynamic effect of flooding on ecosystems' carbon cycle especially under global climate change.

4.3 Microbial and abiotic contributions to carbon capture in riparian zones

While our research suggests that vegetation is a major factor in defining carbon fluxes, microbial organisms likely bring a significant contribution to our results, too. The carbon sequestration of bare soil decreased from pre-flooding season to post-flooding season. It can be attributed to the fact that inundation periods increases soil enzyme activities (Geng *et al.*, 2017, Ou *et al.*, 2019), active bacterial counts, and respiration rates (Anderson *et al.*, 2020, Ou *et al.*, 2019). The aerobic conditions during wet-dry cycles could increase the decomposition of stored organic matter in soils (Denef *et al.*, 2001, Marín-Muñiz *et*

https://doi.org/10.5194/bg-2022-175
Preprint. Discussion started: 29 August 2022

al., 2015). A previous study found that after 25 days of soil moisture enhancement, the anaerobiosis stimulates CO_2 loss by 1.5 times more than the normal soil moisture environment (Huang & Hall, 2017). Flooding leads to elevated soil moisture for weeks or even months, and thus the bare soil after flooding may show an accelerated CO_2 emission.

4.4 Riparian zones are seasonal areas of high carbon capture

Hydrological flow has been found to be an essential factor within the carbon cycle of various ecosystems (Zarnetske et al., 2018). Our data confirms this, as discussed in both Sect. 4.1 and Sect. 4.2. It would influence not only the river carbon emission but also the terrestrial carbon emission. The water flow and terrestrial vegetation combined making the riparian zone a dynamic carbon pool.

After flooding disturbance, the riparian zone turns from a carbon source to a carbon sink mainly due to vegetation's increased CO_2 capture efficiency and river's also capturing carbon. Though riparian zone is found to be a carbon source in both pre- and post-flooding seasons, with flooding disturbance, the riparian zone has a chance to achieve carbon neutralization at a yearly level. Based on the carbon offset model, we can evaluate the annual CO_2 flux of the riparian zone and evaluate the potential for a certain riparian zone to be a carbon sink. The post-disturbance riparian zone shows huge potential in carbon capture compared with global forest, which is a large and persistent carbon sink with an annual magnitude of 2.4 ± 0.4 Gt C yr^{-1} (Pan et al., 2011). After considering the emissions of forest degradation, the global forest-atmosphere CO_2 flux is estimated to be -5.8 Gt CO_2 yr^{-1} (Harris et al., 2021). Global riparian zone after flooding disturbance, with an estimated global area of 468,000 km^2, can fix up to 0.53 Gt more CO_2. It is larger than the net carbon flux in the rainforest in the Amazon river basin (0.10 CO_2e Gt per year) (Harris et al., 2021). Additionally, the riparian zone after flooding disturbance was found to have a higher carbon sequestration efficiency, which is consistent with previous research (Hastie *et al.*, 2019). Its daily average CO_2 flux is -0.57 g m^{-2} d^{-1} (water: -0.62 g m^{-2} d^{-1}, terrestrial area: -0.455 g m^{-2} d^{-1} without vegetation; -0.680 g m^{-2} d^{-1} with vegetation), while the forest is -0.39 g m^{-2} d^{-1} (Harris et al., 2021).

Many have discussed the diel variability of CO_2 flux in the riparian zone (Gómez-Gener et al., 2021; Reiman and Xu, 2019). Yet, few studies considered the positive effects of flooding season on the carbon cycle and may overestimate the CO_2 emissions. Previous research has found that the nocturnal CO_2 emissions are on average 27% (0.9 gC m^{-2} d^{-1}) greater than those estimated from diurnal concentrations alone (Gómez-Gener et al., 2021). Ignoring night-time CO_2 emissions may underestimate global estimates of carbon emission from running waters to the atmosphere by 0.20–0.55 PgC yr^{-1} (Gómez-Gener et al., 2021). Tiegs et al. 2019 found that the biomes in riparian zones have distinct carbon processing signatures around the earth, but they mainly analysed sites that are relatively free of human impacts (Tiegs et al., 2019).

https://doi.org/10.5194/bg-2022-175
Preprint. Discussion started: 29 August 2022

5 Conclusions

Under global warming, both the risk and the number of flooding event are rising. Our analysis reinforces the need to consider post-disturbance recovered vegetation in riparian zone as a climate mitigation strategy. The recovery of survived riparian vegetation from flooding disturbance can limit overall carbon emission and help neutralize the carbon emissions caused by flooding. Flooding also improves the resource hunting ability of water area, which turns the riparian zone from a carbon source to a carbon sink. 0.53 $Gt \cdot year^{-1}$ more CO_2 is captured because of the flooding, which is 9.1 % of the total CO_2 flux of global forest. This study highlights that carbon-conscious conservation efforts in post-flooding season should promote the establishment of high densities of specific plant species that are both flooding-resistant and efficient at capturing carbon.

https://doi.org/10.5194/bg-2022-175
Preprint. Discussion started: 29 August 2022

Appendix A

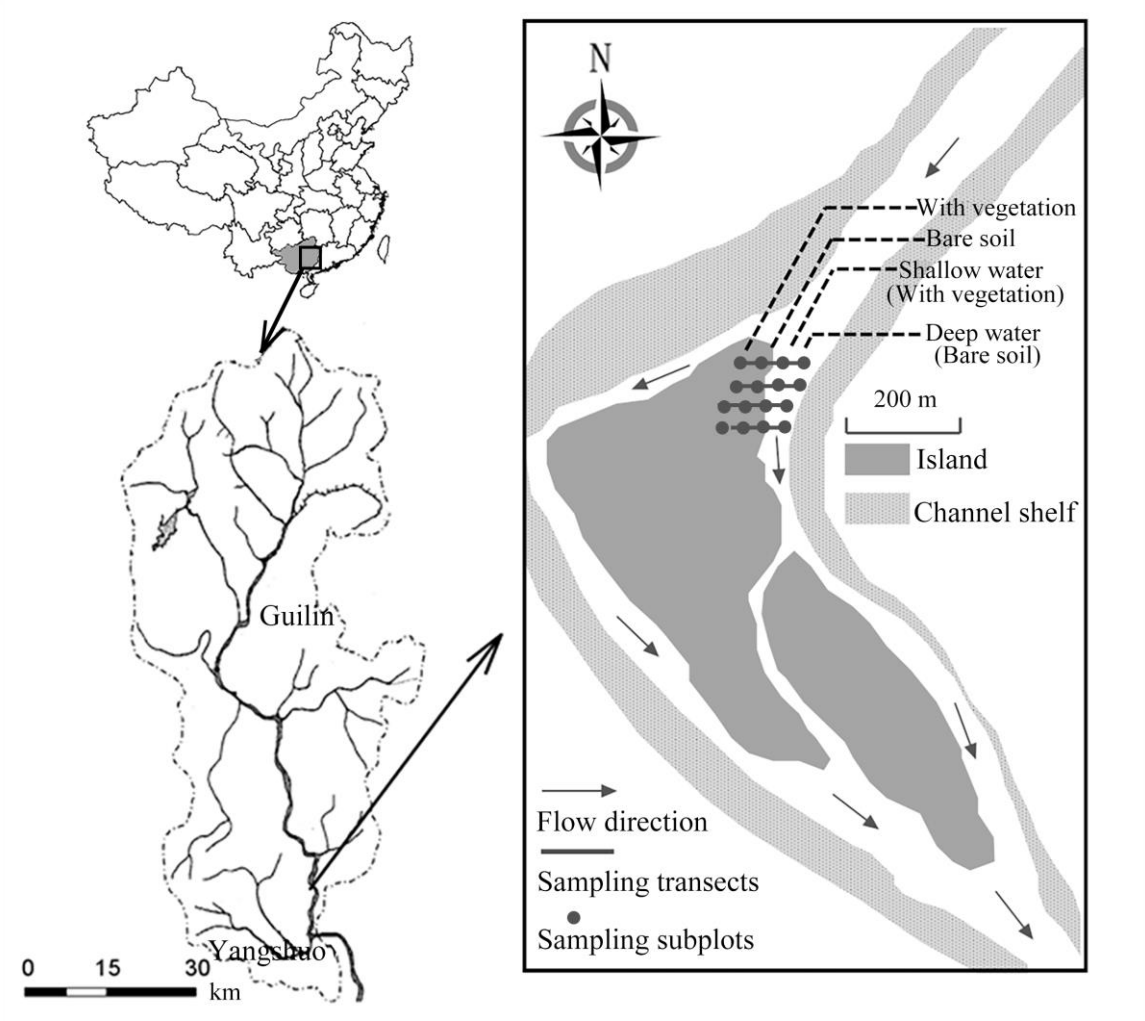

Appendix Figure A1: The location of the study site in the island downstream of Lijiang River in Guilin city, southwest China (25° 06′ N, 110° 25′ E). There were four sampling transects (black lines), each spaced 3 m, and four subplots (black squares) were arranged in each transect, with the distance of 5-8 m between each other.

https://doi.org/10.5194/bg-2022-175
Preprint. Discussion started: 29 August 2022

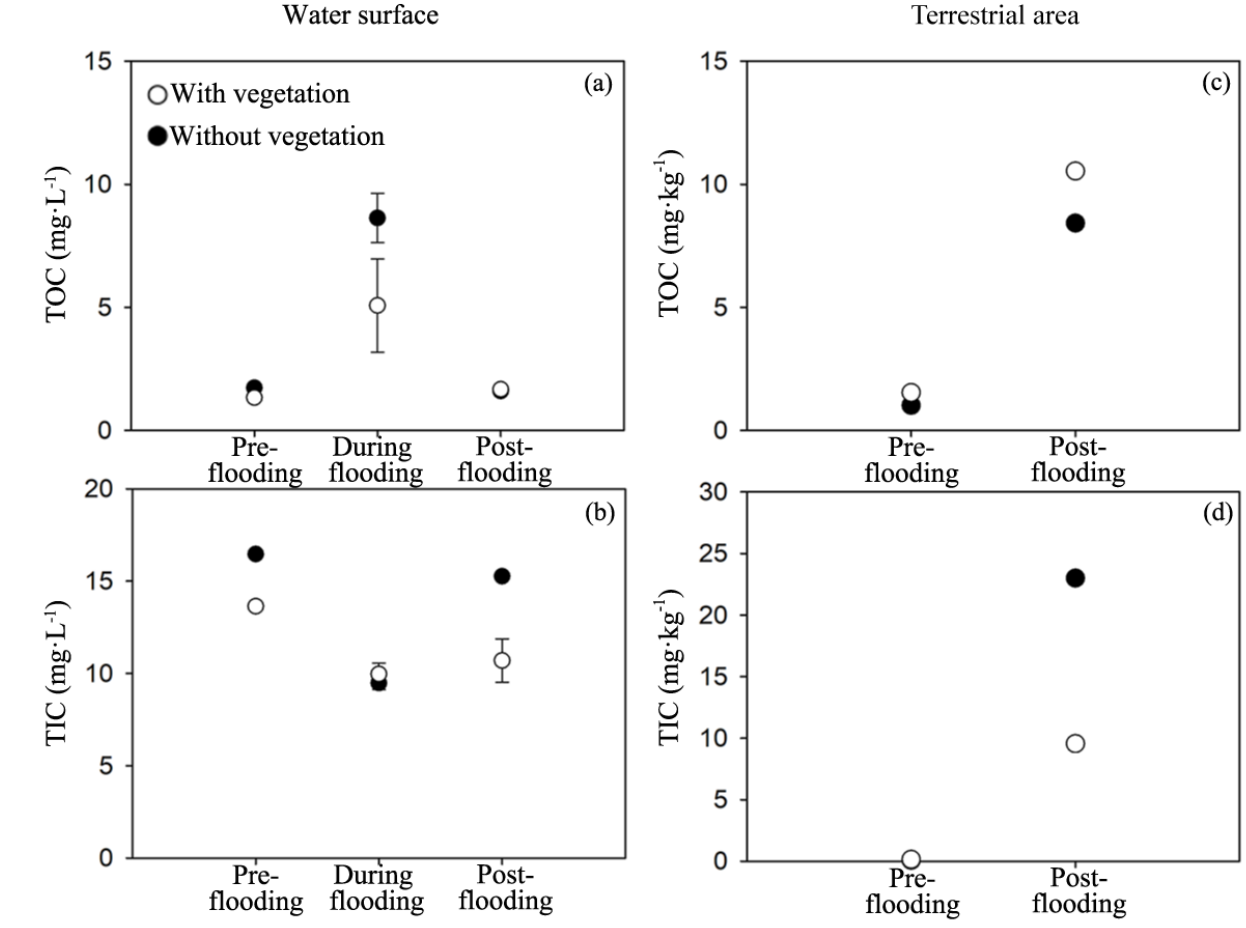

Appendix Figure A2: Total organic carbon (TOC) and total inorganic carbon (TIC) in the study area. The aquatic (water surface) and terrestrial habitats (terrestrial area) include study zones with vegetation and without vegetation. TOC and TIC are also measured in different sampling stages. The ANOVA results for habitats, season, and interaction effects are given, including the degree of freedom (*df*), *F*, and *P* values.

https://doi.org/10.5194/bg-2022-175
Preprint. Discussion started: 29 August 2022

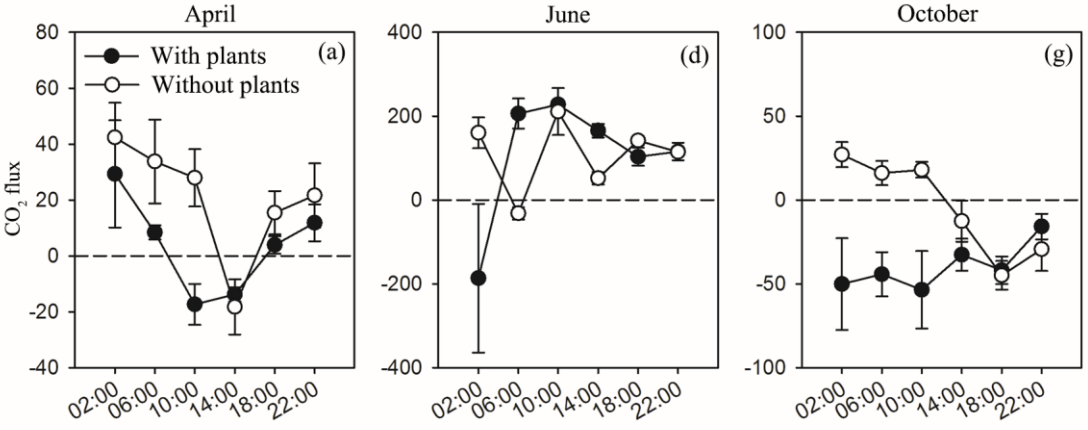

Appendix Figure A3: Effects of time (measuring times in one day) on CO_2 flux in the water surface of the with plants (filled) and without plants (blank) water sections in the three sampling stages. Mean ± 1 SE is given.

Appendix Table A1 ANOVA results for effects of vegetation (with vegetation vs. without vegetation; between-subject factor), sampling seasons (pre-flooding, during flooding, post-flooding), and interaction effects on CO_2 fluxes in two positions (water surface vs. terrestrial area). Degree of freedom (*df*), *F*, and *P* (significance) values are given.

	Water surface				Terrestrial area			
	$F_{1,8}$	*P*	$F_{1,8}$	*P*	$F_{1,8}$	*P*	$F_{1,8}$	*P*
Habitat	3.3	0.094	25.8	<0.001	116.8	<0.001	2289.3	<0.001
Season	24.2	<0.001	46.6	<0.001	4515.9	<0.001	13360.4	<0.001
Interaction	2.5	0.0120	10.7	<0.001	42.8	<0.001	2336.7	<0.001

https://doi.org/10.5194/bg-2022-175
Preprint. Discussion started: 29 August 2022

Data Availability

The data that support the findings of this study are available on the request from the corresponding author.

Author contributions

RL conceived, designed the study, and collected the data with FY. YZ analysed the data, completed data visualization. YZ and RL wrote the original manuscript. HZ, SL, TGG reviewed and edited the manuscript. HZ acquired funding and resources for this study.

Competing interests

The authors declare that they have no conflict of interest.

Disclaimer

Publisher's note: Copernicus Publications remains neutral with regard to jurisdictional claims in published maps and institutional affiliations.

Funding

This research is supported by the National Science Foundation of China (41725017). It is also partially supported by the Strategic Priority Research Program (B) of the Chinese Academy of Sciences (XDB18010202).

Acknowledgements

We are grateful to the fishermen Qiaolian Huang, Yuhua Chen, and Fengzhan Xu along the Lijiang River for their assistance in the overnight field sampling. We also thank Songlin Liu and Maolin Gan at South China Sea Institute of Oceanology, Chinese Academy of Sciences, for supporting TIC and TOC measurements.

References

Allen, G. H. and Pavelsky, T. M.: Global extent of rivers and streams, Science, 361, 585–588, https://doi.org/10.1126/science.aat0636, 2018a.

https://doi.org/10.5194/bg-2022-175
Preprint. Discussion started: 29 August 2022

Allen, G. H. and Pavelsky, T. M.: Global River Widths from Landsat (GRWL) Database, https://doi.org/10.5281/zenodo.1297434, 2018b.

Anderson, N. J., Heathcote, A. J., Engstrom, D. R., and Globocarb data contributors: Anthropogenic alteration of nutrient supply increases the global freshwater carbon sink, Sci. Adv., 6, eaaw2145, https://doi.org/10.1126/sciadv.aaw2145, 2020.

Brienen, R. J. W., Caldwell, L., Duchesne, L., Voelker, S., Barichivich, J., Baliva, M., Ceccantini, G., Di Filippo, A., Helama, S., Locosselli, G. M., Lopez, L., Piovesan, G., Schöngart, J., Villalba, R., and Gloor, E.: Forest carbon sink neutralized by pervasive growth-lifespan trade-offs, Nat Commun, 11, 4241, https://doi.org/10.1038/s41467-020-17966-z, 2020.

Bullock, J. M., Aronson, J., Newton, A. C., Pywell, R. F., and Rey-Benayas, J. M.: Restoration of ecosystem services and biodiversity: conflicts and opportunities, Trends in Ecology & Evolution, 26, 541–549, https://doi.org/10.1016/j.tree.2011.06.011, 2011.

Colmer, T. D., Voesenek, L. a. C. J., Colmer, T. D., and Voesenek, L. a. C. J.: Flooding tolerance: suites of plant traits in variable environments, Functional Plant Biol., 36, 665–681, https://doi.org/10.1071/FP09144, 2009.

Darrel Jenerette, G. and Lal, R.: Hydrologic sources of carbon cycling uncertainty throughout the terrestrial-aquatic continuum, Global Change Biol, 0, 1873–1882, https://doi.org/10.1111/j.1365-2486.2005.01021.x, 2005.

Dynesius, M. and Nilsson, C.: Fragmentation and Flow Regulation of River Systems in the Northern Third of the World, Science, 266, 753–762, https://doi.org/10.1126/science.266.5186.753, 1994.

Elias, E., Steele, C., Havstad, K., Steenwerth, K., Chambers, J., Deswood, H., Kerr, A., Albert, R., Schwartz, M., Stine, P., and Steele, R.: Southwest Regional Climate Hub and California Subsidiary Hub assessment of climate change vulnerability and adaptation and mitigation strategies, 2015.

Gatti, L. V., Basso, L. S., Miller, J. B., Gloor, M., Gatti Domingues, L., Cassol, H. L. G., Tejada, G., Aragão, L. E. O. C., Nobre, C., Peters, W., Marani, L., Arai, E., Sanches, A. H., Corrêa, S. M., Anderson, L., Von Randow, C., Correia, C. S. C., Crispim, S. P., and Neves, R. A. L.: Amazonia as a carbon source linked to deforestation and climate change, Nature, 595, 388–393, https://doi.org/10.1038/s41586-021-03629-6, 2021.

Gómez-Gener, L., Rocher-Ros, G., Battin, T., Cohen, M. J., Dalmagro, H. J., Dinsmore, K. J., Drake, T. W., Duvert, C., Enrich-Prast, A., Horgby, Å., Johnson, M. S., Kirk, L., Machado-Silva, F., Marzolf, N. S., McDowell, M. J., McDowell, W. H., Miettinen, H., Ojala, A. K., Peter, H., Pumpanen, J., Ran, L., Riveros-Iregui, D. A., Santos, I. R., Six, J., Stanley, E. H., Wallin, M. B., White, S. A., and Sponseller, R. A.: Global carbon dioxide efflux from rivers enhanced by high nocturnal emissions, Nat. Geosci., 14, 289–294, https://doi.org/10.1038/s41561-021-00722-3, 2021.

Gregory, S. V., Swanson, F. J., McKee, W. A., and Cummins, K. W.: An Ecosystem Perspective of Riparian Zones, BioScience, 41, 540–551, https://doi.org/10.2307/1311607, 1991.

Harris, N. L., Gibbs, D. A., Baccini, A., Birdsey, R. A., de Bruin, S., Farina, M., Fatoyinbo, L., Hansen, M. C., Herold, M., Houghton, R. A., Potapov, P. V., Suarez, D. R., Roman-Cuesta, R. M., Saatchi, S. S., Slay, C. M., Turubanova, S. A., and Tyukavina, A.: Global maps of twenty-first century forest carbon fluxes, Nat. Clim. Chang., 11, 234–240, https://doi.org/10.1038/s41558-020-00976-6, 2021.

Hassanzadeh, Vidon, Gold, Pradhanang, and Lowder: RZ-TRADEOFF: A New Model to Estimate Riparian Water and Air Quality Functions, Water, 11, 769, https://doi.org/10.3390/w11040769, 2019.

Hirabayashi, Y., Mahendran, R., Koirala, S., Konoshima, L., Yamazaki, D., Watanabe, S., Kim, H., and Kanae, S.: Global flood risk under climate change, Nature Clim Change, 3, 816–821, https://doi.org/10.1038/nclimate1911, 2013.

Hirota, M., Senga, Y., Seike, Y., Nohara, S., and Kunii, H.: Fluxes of carbon dioxide, methane and nitrous oxide in two contrastive fringing zones of coastal lagoon, Lake Nakaumi, Japan, Chemosphere, 68, 597–603, https://doi.org/10.1016/j.chemosphere.2007.01.002, 2007.

Hondula, K. L., Jones, C. N., and Palmer, M. A.: Effects of seasonal inundation on methane fluxes from forested freshwater wetlands, Environ. Res. Lett., 16, 084016, https://doi.org/10.1088/1748-9326/ac1193, 2021.

Li, X., Shi, F., Ma, Y., Zhao, S., and Wei, J.: Significant winter CO_2 uptake by saline lakes on the Qinghai-Tibet Plateau, Global Change Biology, 28, 2041–2052, https://doi.org/10.1111/gcb.16054, 2022.

Liu, X., Lu, X., Yu, R., Sun, H., Xue, H., Qi, Z., Cao, Z., Zhang, Z., and Liu, T.: Greenhouse gases emissions from riparian wetlands: an example from the Inner Mongolia grassland region in China, Biogeosciences, 18, 4855–4872, https://doi.org/10.5194/bg-18-4855-2021, 2021.

Luo, F.-L., Chen, Y., Huang, L., Wang, A., Zhang, M.-X., and Yu, F.-H.: Shifting effects of physiological integration on performance of a clonal plant during submergence and de-submergence, Annals of Botany, 113, 1265–1274, https://doi.org/10.1093/aob/mcu057, 2014.

Mahanta, S. K., Ghosh, P. K., and Ramakrishnan, S.: Tropical Grasslands as Potential Carbon Sink, in: Carbon Management in Tropical and Sub-Tropical Terrestrial Systems, edited by: Ghosh, P. K., Mahanta, S. K., Mandal, D., Mandal, B., and Ramakrishnan, S., Springer, Singapore, 299–311, https://doi.org/10.1007/978-981-13-9628-1_18, 2020.

Maraseni, T. N. and Cockfield, G.: Crops, cows or timber? Including carbon values in land use choices, Agriculture, Ecosystems & Environment, 140, 280–288, https://doi.org/10.1016/j.agee.2010.12.015, 2011.

Maraseni, T. N. and Mitchell, C.: An assessment of carbon sequestration potential of riparian zone of Condamine Catchment, Queensland, Australia, Land Use Policy, 54, 139–146, https://doi.org/10.1016/j.landusepol.2016.02.013, 2016.

Morse, J. L., Ardón, M., and Bernhardt, E. S.: Greenhouse gas fluxes in southeastern U.S. coastal plain wetlands under contrasting land uses, Ecological Applications, 22, 264–280, https://doi.org/10.1890/11-0527.1, 2012.

Naiman, R. J. and Decamps, H.: The Ecology of Interfaces: Riparian Zones, Annual Review of Ecology and Systematics, 28, 621–658, 1997.

Pan, Y., Birdsey, R. A., Fang, J., Houghton, R., Kauppi, P. E., Kurz, W. A., Phillips, O. L., Shvidenko, A., Lewis, S. L., Canadell, J. G., Ciais, P., Jackson, R. B., Pacala, S. W., McGuire, A. D., Piao, S., Rautiainen, A., Sitch, S., and Hayes, D.: A Large and Persistent Carbon Sink in the World's Forests, Science, 333, 988–993, https://doi.org/10.1126/science.1201609, 2011.

Pugh, T. A. M., Arneth, A., Kautz, M., Poulter, B., and Smith, B.: Important role of forest disturbances in the global biomass turnover and carbon sinks, Nat Geosci, 12, 730–735, https://doi.org/10.1038/s41561-019-0427-2, 2019.

Reiman, J. H. and Xu, Y. J.: Diel Variability of pCO2 and CO2 Outgassing from the Lower Mississippi River: Implications for Riverine CO2 Outgassing Estimation, Water, 11, 43, https://doi.org/10.3390/w11010043, 2019.

Ren, Y., Wang, D., and Li, X.: Impacts of Human Disturbances on Riparian Herbaceous Communities in a Chinese Karst River, Nature Environment and Pollution Technology, 18, 1107–1118, 2019.

https://doi.org/10.5194/bg-2022-175
Preprint. Discussion started: 29 August 2022

Running, S. W.: Ecosystem Disturbance, Carbon, and Climate, Science, 321, 652–653, https://doi.org/10.1126/science.1159607, 2008.

Sierra, C. A., Müller, M., Metzler, H., Manzoni, S., and Trumbore, S. E.: The muddle of ages, turnover, transit, and residence times in the carbon cycle, Glob Change Biol, 23, 1763–1773, https://doi.org/10.1111/gcb.13556, 2017.

Steiger, J., Tabacchi, E., Dufour, S., Corenblit, D., and Peiry, J.-L.: Hydrogeomorphic processes affecting riparian habitat within alluvial channel-floodplain river systems: a review for the temperate zone, River Res. Applic., 21, 719–737, https://doi.org/10.1002/rra.879, 2005.

Still, C. J., Berry, J. A., Collatz, G. J., and DeFries, R. S.: Global distribution of C_3 and C_4 vegetation: Carbon cycle implications: C_4 PLANTS AND CARBON CYCLE, Global Biogeochem. Cycles, 17, 6-1-6–14, https://doi.org/10.1029/2001GB001807, 2003.

Tiegs, S. D., Costello, D. M., Isken, M. W., Woodward, G., McIntyre, P. B., Gessner, M. O., Chauvet, E., Griffiths, N. A., Flecker, A. S., Acuña, V., Albariño, R., Allen, D. C., Alonso, C., Andino, P., Arango, C., Aroviita, J., Barbosa, M. V. M., Barmuta, L. A., Baxter, C. V., Bell, T. D. C., Bellinger, B., Boyero, L., Brown, L. E., Bruder, A., Bruesewitz, D. A., Burdon, F. J., Callisto, M., Canhoto, C., Capps, K. A., Castillo, M. M., Clapcott, J., Colas, F., Colón-Gaud, C., Cornut, J., Crespo-Pérez, V., Cross, W. F., Culp, J. M., Danger, M., Dangles, O., de Eyto, E., Derry, A. M., Villanueva, V. D., Douglas, M. M., Elosegi, A., Encalada, A. C., Entrekin, S., Espinosa, R., Ethaiya, D., Ferreira, V., Ferriol, C., Flanagan, K. M., Fleituch, T., Follstad Shah, J. J., Frainer, A., Friberg, N., Frost, P. C., Garcia, E. A., García Lago, L., García Soto, P. E., Ghate, S., Giling, D. P., Gilmer, A., Gonçalves, J. F., Gonzales, R. K., Graça, M. A. S., Grace, M., Grossart, H.-P., Guérold, F., Gulis, V., Hepp, L. U., Higgins, S., Hishi, T., Huddart, J., Hudson, J., Imberger, S., Iñiguez-Armijos, C., Iwata, T., Janetski, D. J., Jennings, E., Kirkwood, A. E., Koning, A. A., Kosten, S., Kuehn, K. A., Laudon, H., Leavitt, P. R., Lemes da Silva, A. L., Leroux, S. J., LeRoy, C. J., Lisi, P. J., MacKenzie, R., Marcarelli, A. M., Masese, F. O., McKie, B. G., Oliveira Medeiros, A., Meissner, K., Miliša, M., Mishra, S., Miyake, Y., Moerke, A., et al.: Global patterns and drivers of ecosystem functioning in rivers and riparian zones, Sci. Adv., 5, eaav0486, https://doi.org/10.1126/sciadv.aav0486, 2019.

Venter, O., Sanderson, E. W., Magrach, A., Allan, J. R., Beher, J., Jones, K. R., Possingham, H. P., Laurance, W. F., Wood, P., Fekete, B. M., Levy, M. A., and Watson, J. E. M.: Sixteen years of change in the global terrestrial human footprint and implications for biodiversity conservation, Nat Commun, 7, 12558, https://doi.org/10.1038/ncomms12558, 2016.

Wang, J., Wang, D., Ren, Y., and Wang, B.: Coupling relationships between soil microbes and soil nutrients under different hydrologic conditions in the riparian zone of the Lijiang River, Acta Ecol. Sin, 39, https://doi.org/10.5846/stxb201803260595, 2019.

Wang, J., Feng, L., Palmer, P. I., Liu, Y., Fang, S., Bösch, H., O'Dell, C. W., Tang, X., Yang, D., Liu, L., and Xia, C.: Large Chinese land carbon sink estimated from atmospheric carbon dioxide data, Nature, 586, 720–723, https://doi.org/10.1038/s41586-020-2849-9, 2020.

Wei, G.-W., Shu, Q., Luo, F.-L., Chen, Y.-H., Dong, B.-C., Mo, L.-C., Huang, W.-J., and Yu, F.-H.: Separating effects of clonal integration on plant growth during submergence and de-submergence, Flora, 246–247, 118–125, https://doi.org/10.1016/j.flora.2018.08.004, 2018.

Xunhua, Z., Mingxing, W., Yuesi, W., Renxing, S., Jing, L., Heyer, J., Kogge, M., Laotu, L., and Jisheng, J.: Comparison of manual and automatic methods for measurement of methane emission from rice paddy fields, Adv. Atmos. Sci., 15, 569–579, https://doi.org/10.1007/s00376-998-0033-5, 1998.

https://doi.org/10.5194/bg-2022-175
Preprint. Discussion started: 29 August 2022

Zarnetske, J. P., Bouda, M., Abbott, B. W., Saiers, J., and Raymond, P. A.: Generality of Hydrologic Transport Limitation of Watershed Organic Carbon Flux Across Ecoregions of the United States, Geophys. Res. Lett., 45, https://doi.org/10.1029/2018GL080005, 2018.